Journal of Power Sources 214 (2012) 166–170

Contents lists available at SciVerse ScienceDirect

Journal of Power Sources

journal homepage: www.elsevier.com/locate/jpowsour

Short communication

Challenges toward higher temperature operation of $LiFePO_4$

Tomochika Kurita [a,b], Jiechen Lu [a], Makoto Yaegashi [a], Yuki Yamada [a], Shin-ichi Nishimura [a], Tsutomu Tanaka [b], Takuya Uzumaki [b], Atsuo Yamada [a,*]

[a] Department of Chemical System Engineering, School of Engineering, The University of Tokyo, 7-3-1 Hongo, Bunkyo, Tokyo 113-8656, Japan
[b] Fujitsu Laboratories, Ltd., 10-1 Morinosatowakamiya, Atsugi 243-0197, Japan

HIGHLIGHTS

- Charge–discharge properties of $LiFePO_4$ at 60 °C–115 °C were investigated.
- Elevating temperature up to 100 °C significantly enhanced reaction speed of $LiFePO_4$.
- Side reaction to form resistive surface layer impede high-rate performance above 100 °C.
- Trade-off between fast kinetics and side reaction is to be considered at higher temperature.
- Miscibility gap do not shrink for samples with >40 nm at 115 °C.

ARTICLE INFO

Article history:
Received 28 March 2012
Received in revised form
6 April 2012
Accepted 25 April 2012
Available online 30 April 2012

Keywords:
Lithium iron phosphate
Middle-temperature region
Rate capability
A.C. impedance spectroscopy

ABSTRACT

Large-scale lithium-ion batteries operating at higher temperature may provide additional advantageous aspects such as higher power and use of new materials which are inactive at ambient temperatures. As a first step for this direction, we applied $LiFePO_4$ cathode to middle-temperature region of 60 °C–115 °C and investigated temperature-dependent charge–discharge properties. By selecting suitable electrolyte and battery components tolerant to the elevated temperature, stable operation was attained for no less than 50 cycles below 115 °C. High-rate performance was significantly improved as operating temperature increased up to 100 °C, but suffered from abrupt increase in polarization above 100 °C, where the corresponding impedance signal emerged, which might be assigned to some side reactions occurring at the surface of $LiFePO_4$ particles. At 100 °C, the discharge capacity over 100 mAh g^{-1} was achieved at 200*C* rate, even with 10wt% of carbon in the electrode composite of $LiFePO_4$. Shrinkage of miscibility gap was not confirmed for samples larger than 40 nm at < 115 °C.

1. Introduction

Nowadays, battery is the key component in portable electronics devices. Many researchers are struggled to stuff up more energy and get higher power, without sacrificing stability and safety. Majority of rechargeable batteries in use, e.g., lithium-ion batteries and nickel-hydrogen batteries, operates at room-temperatures, while for large-scale storage at electricity plant, the sodium sulfur (NAS) battery and the sodium/nickel chloride (ZEBRA) battery are equipped, and they operate at high temperatures above 200 °C to maintain electrode materials in molten state and improve ionic conductivity of β-alumina as a Na-conductive electrolyte. On the other hand, there are few reports on batteries operating at middle-temperature range between 60 and 200 °C.

Elevating the battery operation temperature may provide several advantages. We can simply activate the component materials with higher electronic, ionic, and interfacial conductivities, or by passing through different phases upon charge-discharge. This may sometimes lead to the discovery of new materials which are otherwise inactive at ambient temperatures. Negative aspects, however, emerging at elevated temperatures, are decomposition of materials and side reactions occurring at electrode/electrolyte interface.

In this study, the electrode material of our choice was $LiFePO_4$ as it is known as the most stable cathode [1–3]. After identifying separator and electrolyte suitable for tests at elevated temperature, electrode properties were carefully monitored as a function of temperature. Kinetic enhancement and depression were analyzed by impedance spectroscopy to set the maximum temperature for stable operation at high-rate without side reactions.

* Corresponding author. Tel.: +81 3 5841 7295; fax: +81 3 5841 7488.
E-mail address: yamada@chemsys.t.u-tokyo.ac.jp (A. Yamada).

0378-7753/$ – see front matter © 2012 Elsevier B.V. All rights reserved.
doi:10.1016/j.jpowsour.2012.04.073

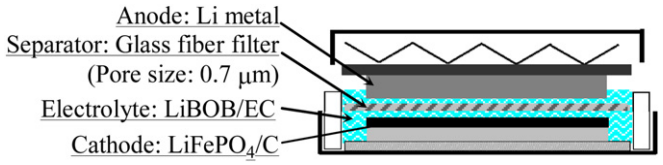

Fig. 1. Cell components selected for higher temperature operation.

2. Experimental

Electrode composite of $LiFePO_4$ were synthesized as a composite with 10wt% (in final product) carbon by solid-state reaction [4] using lithium carbonate (Li_2CO_3, Wako Pure Chemical Industries, 99.9%), iron oxalate ($FeC_2O_4 \cdot 2H_2O$, Junsei Chemical, 99%), and diammonium hydrophosphate ($(NH_4)_2HPO_4$, Wako Pure Chemical Industries, 99%) as precursors, where the carbon is composed of 80wt% ketjen blank ECP® (Lion Corporation) and 20wt% VGCF® (Showa Denko K.K.). The stoichiometric amount of these precursors and additional carbon were mechanically mixed in acetone as a dispersing solvent. Then the solvent was evaporated in vacuum and the residual mixture was calcined for 6 h at 400 °C in argon atmosphere. The final products were analyzed by X-ray diffraction (Bruker AXS D8 ADVANCE equipped with Co Kα radiation, $\lambda = 1.79$Å) and field emission scanning electron microscope (Hitachi High-Technologies S-4800).

Electrochemical cells (CR2032-type) were fabricated to evaluate the charge-discharge performance (Fig. 1). Assembly was carried out in an argon-filled glove box with less than 10ppm moisture. Li metal foil was used as the counter and reference electrode. The electrolyte of our cell was 1 M lithium bis(oxalate)borate (LiBOB) dissolved in ethylene carbonate (Tomiyama Chemicals). LiBOB has been reported to be thermally stable below 300 °C [5] and trial to use with $LiFePO_4$ was already reported [6]. In order to functionalize the electrolyte with high viscosity, a glass fiber filter (Whatman™, GF/F grade with pore size of 0.7 μm) was employed as a separator. Working electrodes were formulated with 95wt% $LiFePO_4$/C composite and 5wt% polyvinylidene fluoride (PVdF) binder, and were spread out on aluminum foil current collectors using N-methylpyrrolidone (NMP) as the solvent. The obtained cathode sheets were dried at 120 °C under vacuum overnight. The sheet with an active material loading amount of 0.53 mg cm^{-2}–0.58 mg cm^{-2}, with thickness of 12 μm–15 μm, was then pressed onto aluminum mesh to form a 16 mmØ disk.

Charge and discharge tests were performed using HJ-SD8 (Hokuto Denko). The cells were galvanostatically charged and discharged over the potential range from 2.0 V to 3.65 V at the 0.5*C* rate prior to subsequent investigations. A constant voltage (3.65 V) relaxation down to 0.05*C* rate current was applied at the end of the charging process to ensure the full-theoretical capacity. Charge-discharge tests were performed at various temperatures (60°C–115 °C) and discharge rates (0.5*C*–200*C*).

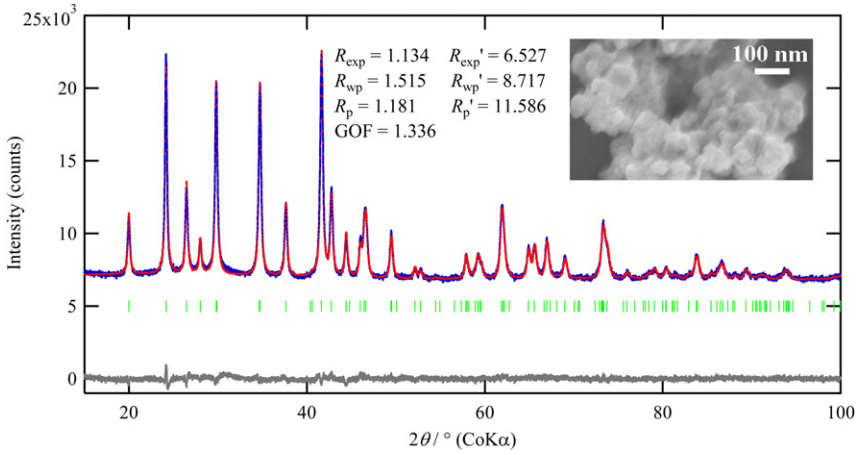

Fig. 2. XRD diffraction pattern of $LiFePO_4$/C composite with Rietveld refinement result. Inset shows typical SEM image.

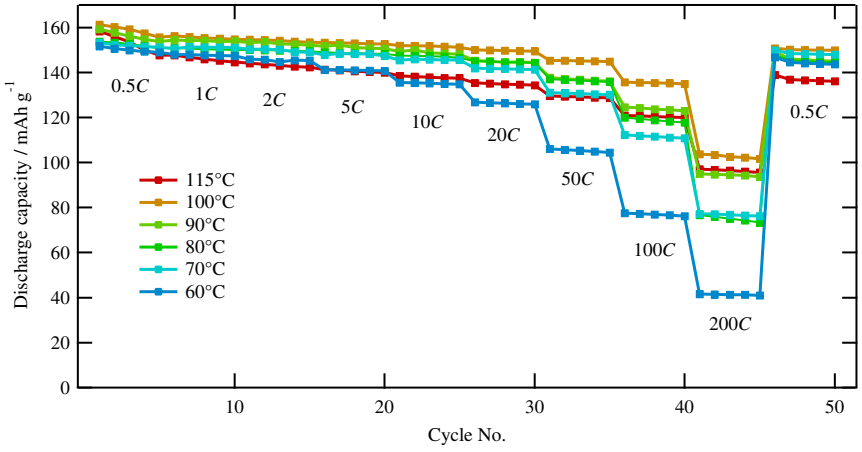

Fig. 3. Temperature dependence of the discharge capacity at each cycle number and various discharge rate.

Temperature-dependent impedance measurement was performed for a coin cell with two-electrode configuration using EC-Lab (Bio-Logic). Applied frequency was varied in a range of 100 kHz–10 mHz, and the applied ac voltage was 7.07 mV (RMS) at open circuit condition.

3. Results and discussions

3.1. Materials characterization

Fig. 2 shows XRD pattern with Rietveld refinement results and SEM image of synthesized $LiFePO_4$/C composite. No impurity was detected with reasonable fitting quality of $R_{wp} = 1.515$, and the primary particle size was estimated to be around 50 nm by both of Rietveld analysis and SEM image.

3.2. Charge–discharge properties

Fig. 3 shows discharge capacities on each cycle number and Fig. 4 shows discharge curves at various rates measured at 60 °C, 100 °C and 115 °C. Voltage profiles at low current rate do not depend on the temperature, and this was also the case for all samples with size of >40 nm. Thereby, shrinkage of miscibility gap [4,7–9] was not confirmed for samples larger than 40 nm at < 115 °C, in contrast to the previous reports that the shrinkage is remarkable even at around 40–50 °C [9]. Up to 100 °C, more than 90% of initial capacity (at 0.5*C*) were retained on the 50th cycle with larger capacity at elevated temperature, being more noticeable at high discharge rate, especially at 100 °C, discharge capacity of >100 mAh g^{-1} was observed at 200*C* rate. However, when the temperature was further increased to 115 °C, only ~86% of discharge capacity of the 1st cycle was maintained on the 50th cycle, with abrupt increase in polarization and less improved rate capability than those at 100 °C. This should be caused by the parasitic internal resistance induced at >100 °C.

3.3. AC impedance measurement

For further investigation on the best performance at 100 °C and abrupt degradation above 100 °C, we performed temperature-dependent a.c. impedance measurement of the cell cycled 10 times at 0.5*C* before measurement.

First of all, we measured impedance spectra at various DOD (0%, 20%, 40%, 60% and 100%) at 30 °C and the results are shown in Fig. 5. No significant difference was found for spectra at the frequency of 100 kHz–10 Hz, at which just one quasi-semicircle was observed, while the spectra at 10 Hz–10 mHz, assigned as solid-state diffusion of Li^+ in $LiFePO_4$ [10], showed DOD dependence. It corresponds to lithium-ion conductivity, simply following the Arrhenius equation at 50°C–230 °C without any degradation [11], thereby the process at 10 Hz–10 mHz is not involved in degradation above 100 °C. Therefore, we will focus on the impedance spectra at 100 kHz–10 Hz, which are independent of DOD. Hereafter, we will discuss the temperature-dependent spectra of DOD = 0% as a representative.

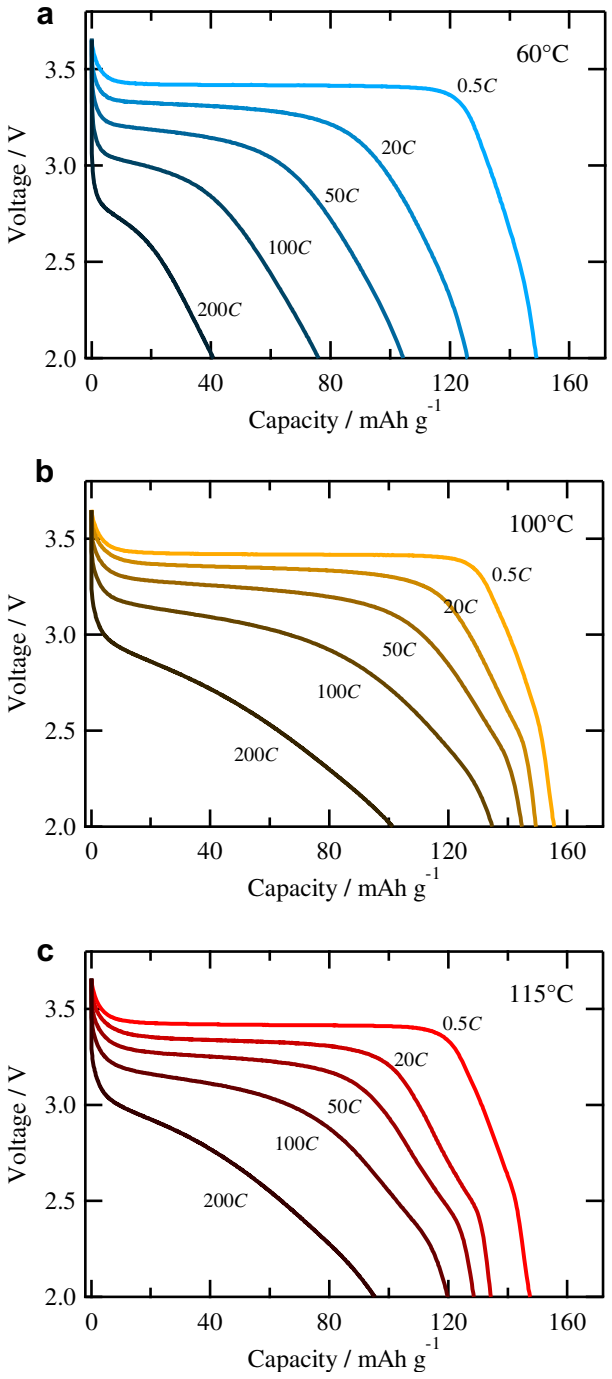

Fig. 4. Discharge profiles at various rates, measured at a) 60 °C, b) 100 °C and c) 115 °C.

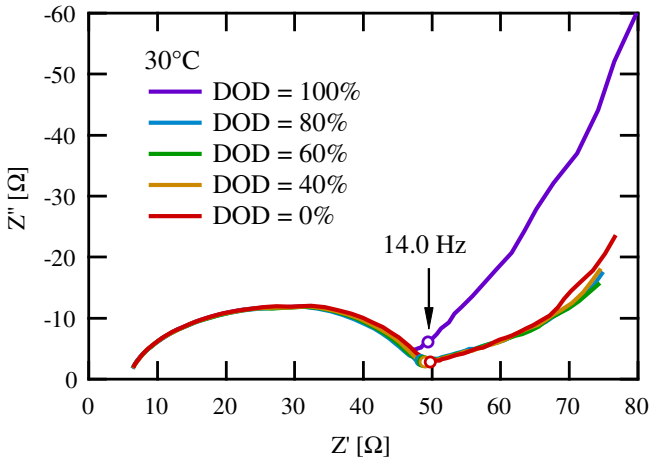

Fig. 5. The impedance spectra of the $LiFePO_4$/electrolyte/Li cell at various depth of discharge (DOD), with the white circles which indicate the frequency of 14.0 Hz.

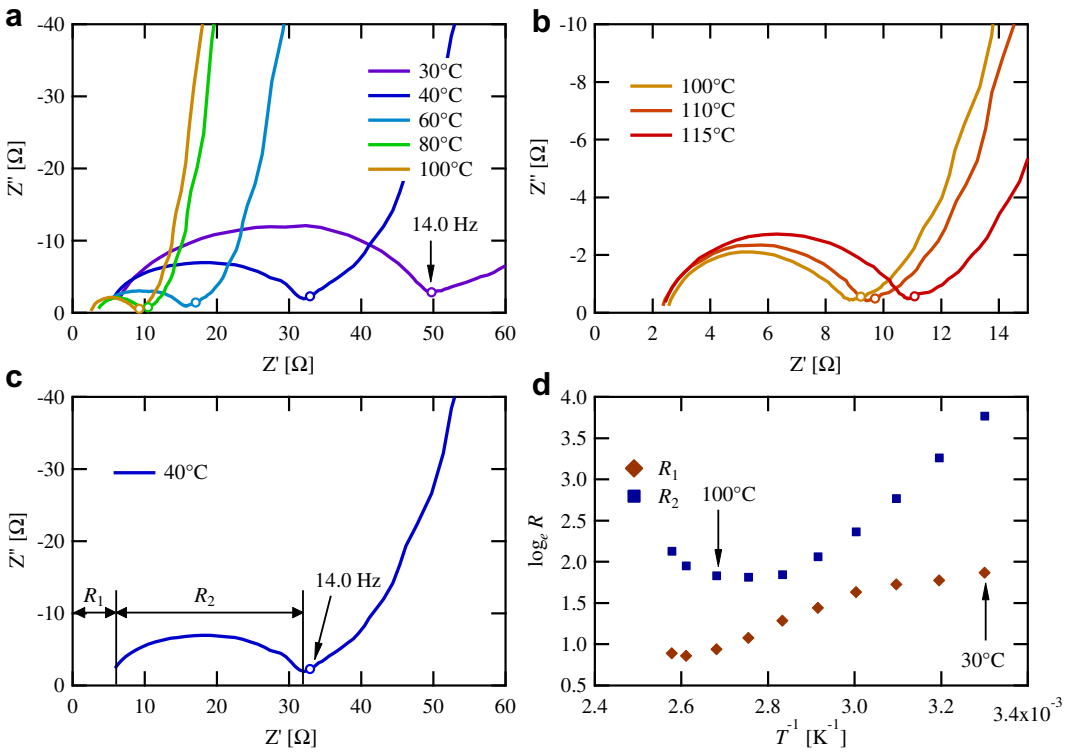

Fig. 6. The impedance spectra of the $LiFePO_4$/electrolyte/Li cell at DOD = 0%. The temperature ranges are a) 30 °C–100 °C, b) 100 °C–115 °C, respectively. The white circle at each spectrum indicates the frequency of 14.0 Hz c) The definitions of R_1 and R_2. d) The temperature dependences of R_1 and R_2.

Fig. 6a and b show the temperature-dependent impedance spectra measured at 30 °C–115 °C. At all temperatures, one quasi-semicircle was present at the frequency range of 10 kHz–10 Hz. Here, we note two resistance values, R_1 and R_2, as defined in Fig. 6c, and their temperature dependences are summarized in Fig. 6d. R_1 decreases as a function of temperature up to 100 °C (Activation energy: 0.13 eV). In general, R_1 indicates the ohmic process such as ionic conductivity of the electrolyte, thereby

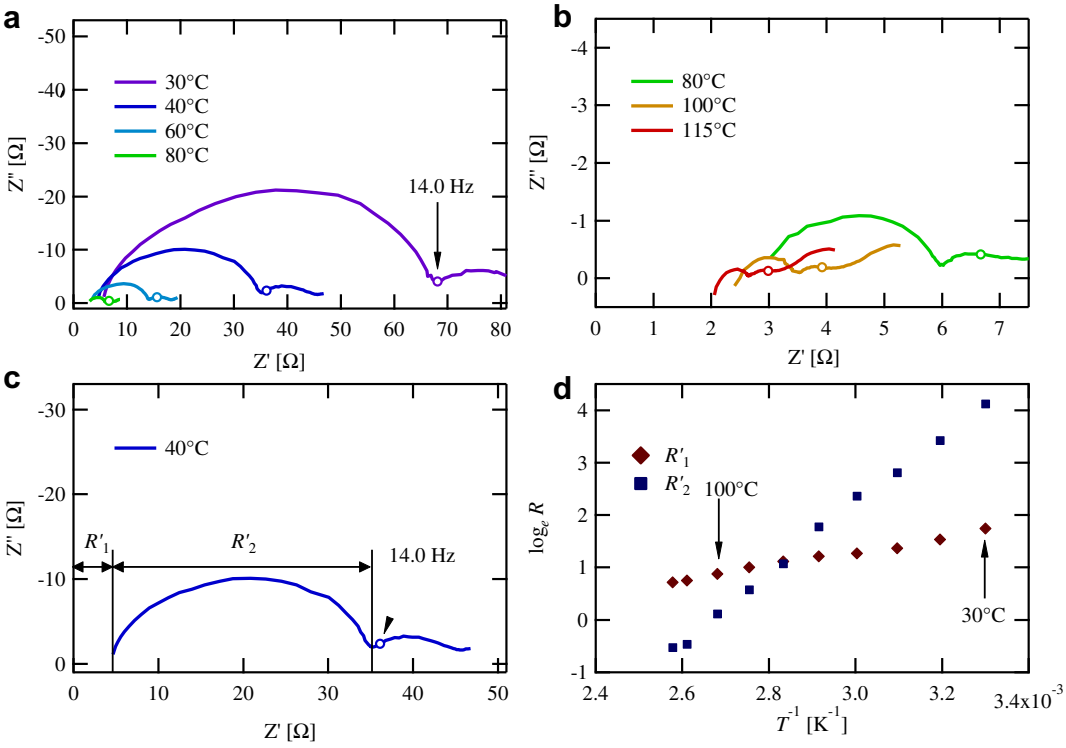

Fig. 7. The impedance spectra of the Li/electrolyte/Li cell. The temperature ranges are a) 30 °C–80 °C, b) 80 °C–115 °C, respectively. The white circle at each spectrum indicates the frequency of 14.0 Hz c) The definitions of R'_1 and R'_2. d) The temperature dependences of R'_1 and R'_2.

monotonic decrease with activation energy of 0.13 V is not surprising. On the other hand, R_2 once decreases up to 80 °C (Activation energy: 0.38 eV) then turns to increase above 80 °C. Therefore, major source of inferior rate capability above 100 °C should be involved in R_2. In order to clarify the contribution from the anode side, we constructed the Li/electrolyte/Li symmetric cell and 10-cycle charges and discharges were performed before impedance measurement at 0.5*C*. The impedance spectra of the Li/electrolyte/Li cell at various temperatures are shown in Fig. 7a and b. One quasi-semicircle was present at the frequency range of 100 kHz–10 Hz at all temperatures, similar to the $LiFePO_4$/electrolyte/Li cell. Here, we note the resistance values R'_1 and R'_2 as defined in Fig. 7c, and their temperature dependences are summarized in Fig. 7d. Contrary to R_2 in the $LiFePO_4$/electrolyte/Li cell, the R'_2 value monotonically decreases over the whole temperature range from 30 °C to 115 °C. The activation energies of R_1 and R_2 were calculated to 0.11 eV and 0.56 eV, respectively. The activation energy of R'_1 was very close to that of R_1, indicating the origin of R_1 is the ionic conduction in the electrolyte. On the other hand, the activation energy of R'_2 was larger than that of R_2, and most importantly, the increase of R'_2 value above 80 °C was not detected, contrary to R_2. This proves that the abrupt increase in R_2 above 80 °C in $LiFePO_4$/electrolyte/Li cell is due to cathode side.

There are three possible cathode processes involved in R_2; (i) ionic transfer at electrolyte/$LiFePO_4$ interface, (ii) electronic transfer at $LiFePO_4$/carbon interface, and (iii) electronic transfer at cathode (carbon)/aluminum sheet interface. In the previous literature, the third one was reported to be almost independent of temperature [10]. Therefore, increase in R_2 above 80 °C occurs at the surface of $LiFePO_4$ particle. As Li_xFePO_4 and LiBOB/EC themselves are both stable against high temperature over 80 °C. Elevated temperature might induce side reaction to form resistive layer between electrode/electrolyte interfaces. Details of the surface layer, including chemical species and formation temperature, will depend on the electrolyte, and needs further investigations towards operation at higher temperatures.

4. Conclusions

Applying LiBOB as electrolyte salt and glass fiber filter as a separator, elevating temperature up to ca. 100 °C was very effective to enhance reaction speed of $LiFePO_4$ electrode, reaching >100 mAh g^{-1} at 200*C* rate with 10wt% carbon in the electrode composite. Surface resistive layer was detected by impedance spectroscopy above 80 °C, which was identified to impede the high-rate operation at >100 °C. Although the strategies to realize higher temperature operation depend on the electrolyte, overall trade-off between fast kinetics and surface side reaction should be taken into account.

References

[1] A.K. Padhi, K.S. Nanjundaswamy, J.B. Goodenough, J. Electrochem. Soc. 144 (1997) 1188–1194.
[2] A. Yamada, S.C. Chung, K. Hinokuma, J. Electrochem. Soc. 148 (2001) A224–A229.
[3] M. Takahashi, S. Tobishima, K. Takei, Y. Sakurai, Solid State Ionics 148 (2002) 283–289.
[4] G. Kobayashi, S. Nishimura, M.-S. Park, R. Kanno, M. Yashima, T. Ida, A. Yamada, Adv. Funct. Mater. 19 (2009) 395–403.
[5] K. Xu, S. Zhang, T.R. Jow, W. Xu, C.A. Angell, Electrochem. Solid-State Lett. 5 (2002) A26–A29.
[6] F. Mestre-Aizpurua, S. Hamelet, C. Masquelier, M.R. Palacin, J. Power Sources 195 (2010) 6897–6901.
[7] A. Yamada, H. Koizumi, N. Sonoyama, R. Kanno, Electrochem. Solid-State Lett. 8 (2005) A409.
[8] A. Yamada, H. Koizumi, S. Nishimura, N. Sonoyama, R. Kanno, M. Yonemura, T. Nakamura, Y. Kobayashi, Nat. Mater. 5 (2006) 357.
[9] N. Meethong, H.-Y.S. Huang, W.C. Carter, Y.-M. Chiang, Electrochem. Solid-State Lett. 10 (2007) A134.
[10] J.P. Schmidt, T. Chrobak, M. Ender, J. Illig, D. Klotz, E. Ivers-Tiffée, J. Power Sources 196 (2011) 5342–5348.
[11] Jiying Li, Wenlong Yao, Steve Martin, David Vaknin, Solid State Ionics 179 (2008) 2016–2019.